

Deep Learning Model for Extensive Smartphone-based Diagnosis and Triage of Cataracts and Multiple Corneal Diseases

Supplementary Materials

Fig. S1. Representative cases of nine categories and annotation.

Fig. S2. Performance of deep learning algorithm to classify corneal diseases/cataracts into nine categories.

Fig. S3. Representative images of correct and incorrect diagnosis by YOLO V.5.

Fig. S4. Representative images of smartphone camera for nine-category classification.

Fig. S5. Detection of corneal diseases with very small lesions or at early stages based on anterior segment images by YOLO V.5.

Table S1. Corneal diseases included in nine categories.

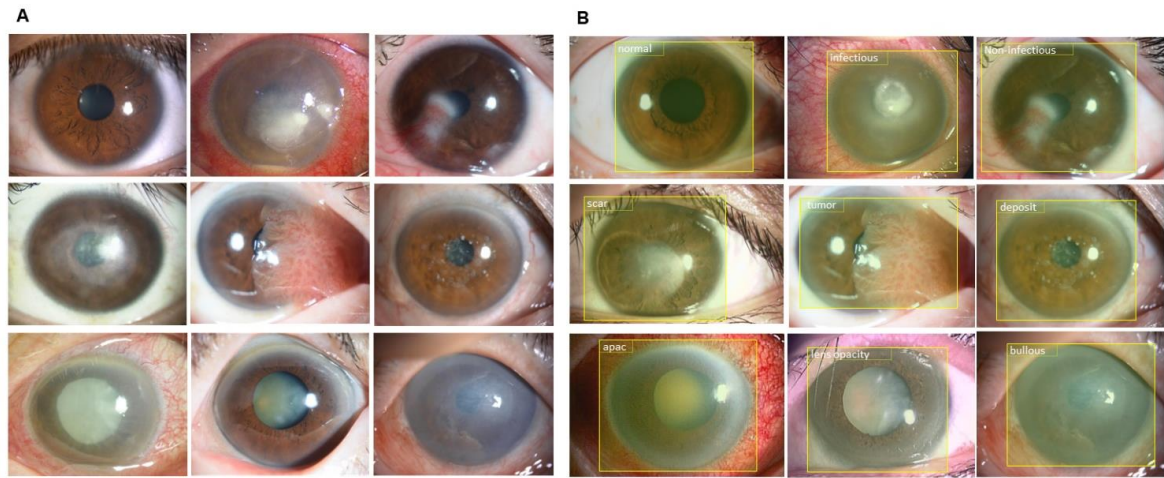
Table S2. Demographics of datasets

Table S3. Demographics of subjects

Table S4. Performance of three deep learning algorithm for nine categories.

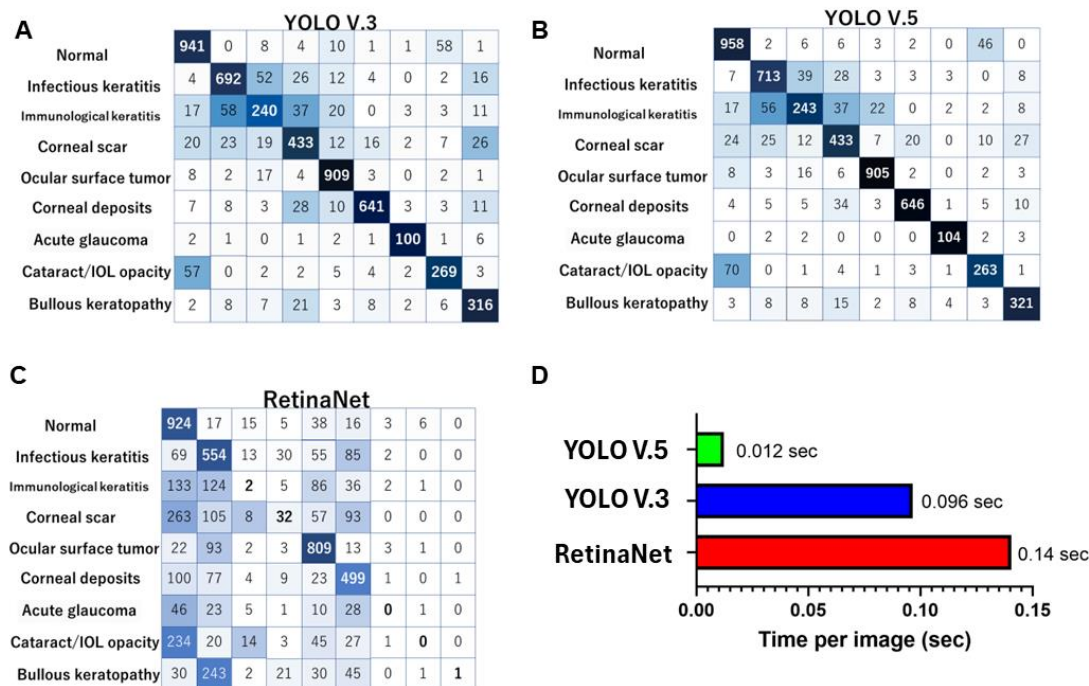
Table S5. Performance of YOLO V.5 in validation datasets.

Table S6. Positive predictive value of classification withing top 3 categories.

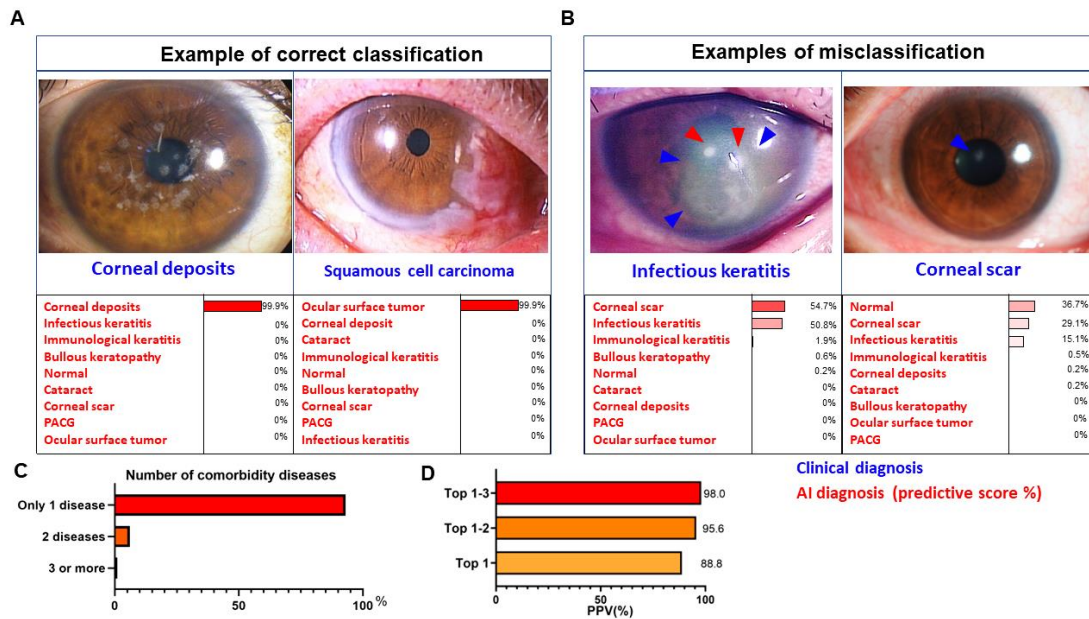
Fig. S1. Representative cases of nine categories and annotation

A, Normal cornea (top left). Infectious keratitis (top middle, bacterial infection of the cornea). Immunological keratitis (top right, phlyctenular keratitis with vascular invasion due to focal inflammation in the center of the cornea). Corneal scar (middle left, corneal opacity after *Pseudomonas aeruginosa* infection). Ocular surface tumor (center, squamous cell carcinoma), Corneal deposits (middle right, granular corneal dystrophy, a kind of hereditary corneal opacity). Primary angle closure glaucoma (down left, glaucoma with elevated intraocular pressure and corneal edema, due to angle closure). Cataracts (down middle, age-related crystalline lens opacity). Bullous keratopathy (down right, corneal endothelial dysfunction results in severe corneal edema). B, Examples of annotations in the images in Fig. S1A.

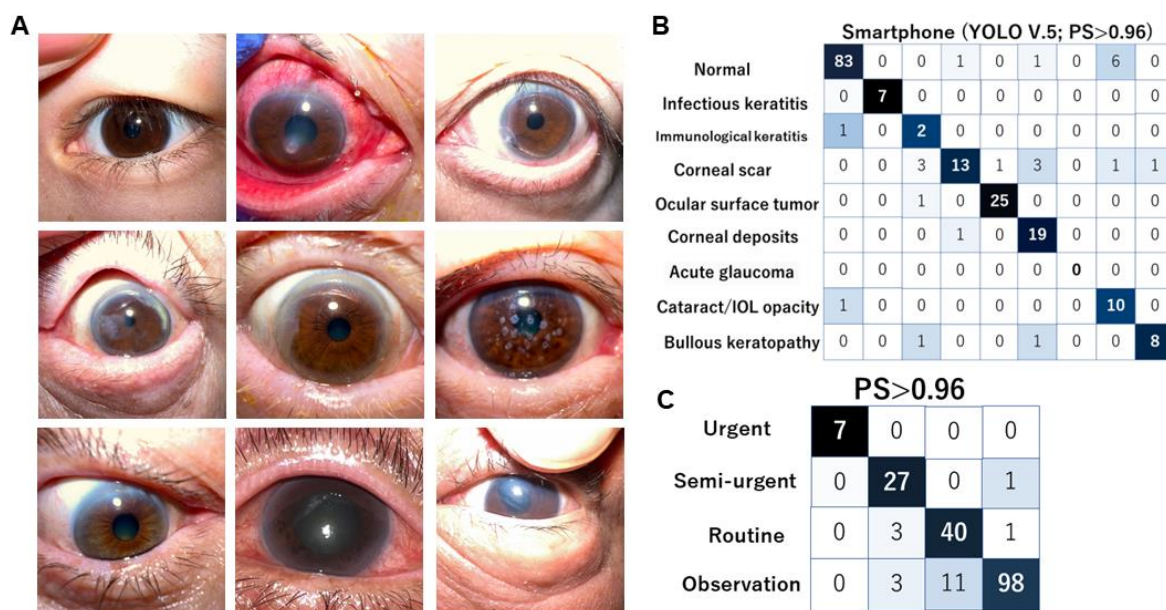
Fig. S2. Performance of deep learning algorithm to classify cornea diseases/cataracts into nine categories.



Performance of three different artificial intelligence (AI) algorithms on a training dataset (5270 images). The confusion matrices of the images show the numbers for the nine categories of three AI algorithms. YOLO V.3 (A), and YOLO V.5 (B) achieved better performances than RetinaNet (C). D, Time to diagnose per image (right) in the three AI algorithm. YOLO V.5 required the least time to complete diagnosis compared to YOLO V.3 and RetinaNet.

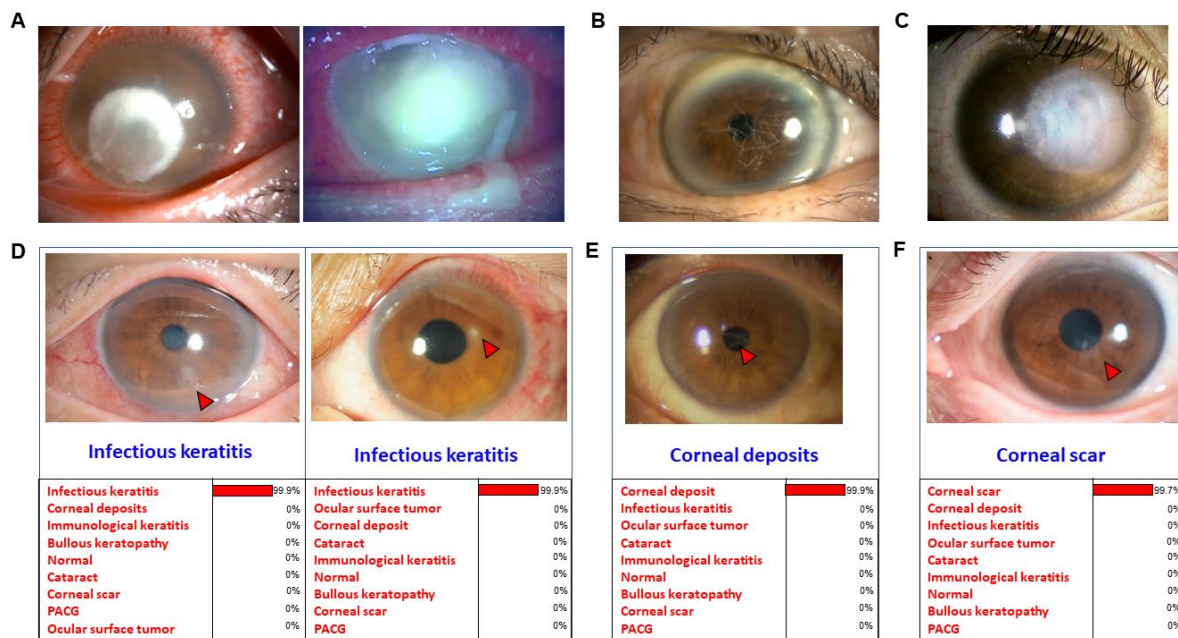
Fig. S3. Representative images of correct and incorrect diagnoses by YOLO V.5.

A, Representative slit-lamp photographs of correct diagnosis had high predictive score of 99.9% (right: corneal scar, left squamous cell carcinoma). B, Presentative slit-lamp photographs with incorrect diagnoses. In the images of infectious keratitis (left), where the infiltration (red arrowheads) got better with the use of antibiotics and scar formation (blue arrowheads) was observed, the predictive score of YOLO V.5 was 54.7% for corneal scar and 50.8% for infectious keratitis. In the images of tiny corneal scars after the resolution of infectious keratitis (right), the predictive score of YOLO V.5 was 36.7% for normal, 29.1% for corneal scar and 15.1% for infectious keratitis. Miscellaneous images with overlapping categories are rare in real-world clinics. C, In the slit-lamp images, two or more categories coexisted in 7%, and 93% had a single category disease. D, The positive predictive value (PPV) increased from 88.8 to 95.6 and 98.0 when the top two or three diseases in predictive score were regarded as correct.

Fig. S4. Representative images of smartphone camera for 9 category classification.

A, Normal cornea. Infectious keratitis (bacterial infection). Immunological keratitis (peripheral ulcerative keratitis). Corneal scar (corneal opacity after herpetic keratitis). Ocular surface tumor (pterygium). Corneal deposits (granular corneal dystrophy). Primary angle closure glaucoma (glaucoma with elevated intraocular pressure and corneal edema, leading to permanent loss of vision within a few days). Cataract. Bullous keratopathy. B, Confusion matrices of image numbers in YOLO V.5 to categorize the nine classifications using smartphone images with a predictive score (PS) of 0.96 or greater. The PPV was 87.4%. C, Confusion matrices of image numbers in triage using smartphone images, stratifying images based on a PS greater than 0.96.

Fig. S5. Detection of corneal diseases with very small lesions or at early stages based only on anterior segment images by YOLO V.5



The AI algorithm can detect corneal diseases with very small or faint lesions at very early stages (red arrowheads). A-C, Representative typical images of infectious keratitis (A), corneal deposits (B, amyloid deposits in hereditary lattice corneal dystrophy type IIIa), and corneal scars after infectious keratitis (C). These images are apparent and are easy for AI and ophthalmologists to diagnose. We expected it to be very difficult for AI to diagnose diseases with small lesions (D, small lesions of infectious keratitis), at a very early stage of the disease (E, hereditary lattice corneal dystrophy type III), and faint lesions (F, corneal scar). However, to our surprise, the YOLO V.5 could detect them with very high predictive score of 99.7 to 99.9%.

Table S1. Corneal diseases which were included in 9 categories.

Categories	
Normal	Normal, Arcus senilis
Infectious keratitis	Bacterial keratitis, Fungal keratitis, Viral keratitis (epithelial dendritic ulcer), Acanthamoeba keratitis
Immunological keratitis	Peripheral ulcerative keratitis (such as Mooren ulcer, and rheumatoid arthritis-related ulcer), Catarrhal keratitis, Phlyctenular keratitis, Meibomian gland associated keratoepitheliopathy, Multiple subepithelial infiltrates, Terrien marginal degeneration (Inflammatory type), Scleritis, stromal keratitis, Shield ulcer (vernal keratoconjunctivitis)
Corneal scar	Corneal scar due to the following reasons: Post-infectious keratitis, Post-immunological keratitis, Post-perforating corneal trauma, Post-ocular surface burns (chemical and thermal), long-standing bullous keratopathy
Ocular surface tumor	Keratoconjunctival tumor (squamous cell carcinoma [SCC], corneoconjunctival intraepithelial neoplasm [CIN], keratolimbic dermoid, conjunctival lymphoma), Pterygium, Pseudopterygium, Conjunctival cyst, Conjunctival nevus, Orbital fat herniation, Pinguecula
Corneal deposits	Band keratopathy, granular corneal dystrophy, lattice corneal dystrophy, macular corneal dystrophy, gelatinous droplet-like dystrophy, corneal amyloidosis (primary/ secondary), Schnyder corneal dystrophy, Reisbuckler corneal dystrophy
PACG	Elevated intraocular pressure due to angle closure
Cataract/IOL opacity	Cataract (including nucleus cataract, cortex cataract, anterior subcapsular cataract, and mature cataract), Posterior capsular opacity after cataract surgery, Anterior capsular opacity, IOL opacity
Bullous keratopathy	Pseudophakic bullous keratopathy, Fuchs endothelial corneal dystrophy, Aphakic bullous keratopathy, Argon-laser-associated bullous keratopathy, Post-glaucoma surgery bullous keratopathy, Irido-cornea endothelial (ICE) syndrome

Definition of each disease; “Cataract” was defined as crystalline lens clouding or opacity. “Infectious keratitis” was defined as a corneal infection due to bacterial, fungal, or acanthamoeba.

“Immunological keratitis” included Mooren’s ulcer, phlyctenular keratitis, corneal marginal ulcer due to rheumatoid arthritis, stromal keratitis, catarrhal keratitis, and shield ulcer. “Corneal scar” was defined as corneal clouding or scarring after corneal inflammation, such as infectious keratitis, immunological keratitis and post-acute-hydrops in advanced keratoconus. “Corneal deposits” included hereditary corneal dystrophies (granular/lattice/macular/gelatinous/ Schnyder dystrophy), band keratopathy, corneal amyloidosis, Fish eye disease, and lipid keratopathy. “Bullous keratopathy” was defined as irreversible corneal edema due to Fuchs corneal endothelial dystrophy or reduced corneal endothelial cells after cataract surgery or laser iridotomy. “Ocular surface tumor” included pterygium, dermoid, squamous cell carcinoma (SCC), corneo-conjunctival intraepithelial neoplasm (CCIN), conjunctival nevus, pinguecula, and lymphoma. Primary angle closure glaucoma (PACG) is an important eye condition, which presents with cataract, elevated intraocular pressure, corneal edema, and hyperemia, and needs to be differentiated from bullous keratopathy. PACG was

defined as acute intraocular pressure rise due to angle closure and pupillary block and included as one category in this study.



Table S2. Demographics of datasets.

	No. of images	Camera	AI model	Age (years)	Female/Male	Detail
9 categories	5270	Slit-lamp	YOLO V.3	61.2±20.4	2799/2446	Normal: 1053 (20.0%)
Training/testing dataset			YOLO V.5	(2-99)	unknown 25	InK: 779 (14.8%)
From 23 tertiary hospitals			RetinaNet			ImK: 389 (7.4%)
						Scar: 558 (10.6%)
						Deposit: 946 (18.0%)
						OST: 714 (13.5%)
						PACG: 114 (2.2%)
						Cataract: 344 (6.5%)
						BK: 373 (7.1%)
Testing dataset	500	Slit-lamp	YOLO V.5	59.8±21.7	253/247	Normal: 83(16.8%)
From 23 tertiary hospitals				(3-94)		InK: 82 (16.4%)
						ImK: 40 (7.8%)
						Scar: 58 (11.6%)
						Deposit: 61 (12.2%)
						OST: 99 (19.8%)
						PACG: 7 (1.4%)
						Cataract: 36 (7.2%)
						BK: 34 (6.8%)
Testing dataset	337	Smartphone	YOLO V.5	NA	NA	Normal: 157 (46.7%)
From 13 tertiary hospitals	336	Slit-lamp				InK: 13(3.9%)
						ImK: 10 (3.0%)
						Scar: 42 (12.5%)
						Deposit: 25 (7.4%)
						OST: 27 (8.0%)
						PACG: 2 (0.6%)
						Cataract: 36 (10.7%)
						BK: 25 (7.4%)

InK: infectious keratitis, ImK: immunological keratitis, PACG: primary angle-closure glaucoma, BK: bullous keratopathy, OST: ocular surface tumor, NA: not available

Table S3. Demographics of subjects

Age	-19	20-29	30-39	40-49	50-59	60-69	70-79	80-	NA
No. of eyes	233	413	370	493	646	1018	1552	1023	22
Male	105	198	198	259	317	504	677	410	
Female	128	215	172	234	329	514	875	613	

NA: not available

	Normal	Infectious keratitis	Immunological keratitis	Corneal scar	Ocular surface tumor	Corneal deposit	Acute angle-closure glaucoma	Cataract/IOL opacity	Bullous keratopathy
Age \pm SD (yo)	55.4 \pm 21.4	53.8 \pm 21.8	55.6 \pm 22.0	56.0 \pm 21.7	63.3 \pm 19.9	67.9 \pm 14.9	72.1 \pm 10.1	72.3 \pm 13.8	73.1 \pm 12.7
Male	492	464	186	327	541	268	40	151	199
Female	602	406	230	275	494	507	81	229	208

IOL: intraocular lens, SD: standard deviation, yo: years old

Table S4. Performance of three deep learning algorithm for nine categories.

	Sensitivity (95% CI)	Specificity (95% CI)	Accuracy (95% CI)
YOLO V.3			
Normal	0.919 (0.901-0.935)	0.972 (0.967-0.977)	0.962 (0.957-0.967)
Infectious keratitis	0.856 (0.830-0.880)	0.978 (0.973-0.982)	0.959 (0.953-0.964)
Immunological keratitis	0.614 (0.567-0.666)	0.978 (0.973-0.982)	0.951 (0.945-0.957)
Corneal scar	0.776 (0.739-0.810)	0.974 (0.969-0.978)	0.953 (0.947-0.959)
Ocular surface tumor	0.961 (0.947-0.972)	0.983 (0.979-0.987)	0.979 (0.975-0.983)
Corneal deposits	0.898 (0.873-0.919)	0.992 (0.989-0.994)	0.979 (0.975-0.983)
Acute angle-closure glaucoma	0.877 (0.803-0.931)	0.997 (0.996-0.999)	0.995 (0.993-0.997)
Cataract/IOL opacity	0.782 (0.735-0.824)	0.983 (0.979-0.987)	0.970 (0.965-0.975)
Bullous keratopathy	0.847 (0.807-0.882)	0.985 (0.981-0.988)	0.975 (0.970-0.979)
YOLO V.5			
Normal	0.936 (0.919-0.950)	0.96.9 (0.963-0.974)	0.962 (0.957-0.967)
Infectious keratitis	0.887 (0.863-0.908)	0.977 (0.973-0.982)	0.964 (0.957-0.968)
Immunological keratitis	0.628 (0.578-0.676)	0.982 (0.978-0.985)	0.956 (0.950-0.961)
Corneal scar	0.776 (0.739-0.810)	0.972 (0.967-0.977)	0.952 (0.945-0.957)
Ocular surface tumor	0.958 (0.943-0.970)	0.991 (0.987-0.993)	0.985 (0.981-0.988)
Corneal deposits	0.906 (0.882-0.926)	0.992 (0.989-0.994)	0.980 (0.976-0.984)
Acute angle-closure glaucoma	0.920 (0.854-0.963)	0.998 (0.996-0.999)	0.996 (0.994-0.998)
Cataract/IOL opacity	0.765 (0.716-0.808)	0.986 (0.982-0.989)	0.971 (0.966-0.976)
Bullous keratopathy	0.863 (0.824-0.896)	0.988 (0.984-0.990)	0.979 (0.974-0.982)
RetinaNet			
Normal	0.902 (0.883-0.920)	0.822 (0.810-0.834)	0.838 (0.828-0.848)
Infectious keratitis	0.686 (0.652-0.718)	0.811 (0.799-0.822)	0.792 (0.780-0.803)
Immunological keratitis	0.005 (0.001-0.018)	0.987 (0.984-0.990)	0.915 (0.907-0.922)
Corneal scar	0.057 (0.040-0.080)	0.984 (0.980-0.987)	0.886 (0.877-0.894)
Ocular surface tumor	0.855 (0.831-0.877)	0.920 (0.912-0.928)	0.909 (0.901-0.916)
Corneal deposits	0.699 (0.664-0.732)	0.925 (0.917-0.932)	0.894 (0.885-0.902)
Acute angle-closure glaucoma	0.000 (0.000-0.032)	0.998 (0.996-0.999)	0.976 (0.972-0.980)
Cataract/IOL opacity	0.000 (0.000-0.011)	0.998 (0.996-0.999)	0.933 (0.926-0.939)
Bullous keratopathy	0.003 (0.000-0.015)	1.000 (0.999-1.000)	0.929 (0.922-0.936)

Table S5. Performance of YOLO V.5

	AUC	95%CI
Normal	0.988	0.992-0.999
Infectious keratitis	0.996	0.978-0.997
Immunological keratitis	0.960	0.925-0.994
Corneal scar	0.987	0.978-0.996
Anterior segment tumor	0.997	0.992-1.000
Corneal deposits	0.993	0.984-1.000
Acute angle-closure glaucoma	1.000	1.000-1.000
Cataract/IOL opacity	0.992	0.985-0.999
Bullous keratopathy	0.993	0.985-1.000

CI: confidence interval, IOL: intraocular lens

Table S6. Positive predictive value of classification within top 3 categories.

	Classification within top 3 categories%	95%CI
Normal	0.951	0.880-0.987
Infectious keratitis	1.000	0.957-1.000
Immunological keratitis	0.949	0.827-0.994
Corneal scar	0.966	0.881-0.996
Anterior segment tumor	1.000	0.963-0.996
Corneal deposits	0.967	0.887-1.000
Acute angle-closure glaucoma	1.000	0.590-1.000
Cataract/IOL opacity	1.000	0.903-0.996
Bullous keratopathy	1.000	0.897-1.000

CI: confidence interval, IOL: intraocular lens